

Masataka Murakami\*, Narihiro Orikasa\*, Mizuho Hoshimoto\*,  
Hiroaki Horie\*\*, Hajime Okamoto\*\*, Hiroshi Kuroiwa\*\*, Haruya Minda\*\*\*, Kenji Nakamura\*\*\*, Sento Nakai\*\*\*\*

\* Meteorological Research Institute, Tsukuba, Japan

\*\* Communications Research Laboratory, Tokyo, Japan

\*\*\* Nagoya University, Nagoya, Japan

\*\*\*\* Nagaoka Institute of Snow and Ice Studies, Nagaoka, Japan

## 1. INTRODUCTION

Various types of disturbances, such as Japan Sea polar-airmass convergence zone(JPCZ), polar low and mesoscale vortex, form and develop over the Japan Sea during cold airmass outbreaks. Cloud systems associated with these disturbances organize on mesoscale and sometimes bring about heavy snowfall on the western side of the Japan Islands. To improve the forecast of snowfall, it is desired to elucidate inner structures and formation/development mechanisms of these disturbances.

In order to investigate inner structures of these disturbances and to clarify their formation /development mechanisms, field campaign "Winter MCSs Observation over the Japan Sea - 2001 (WMO-01)" was carried out in January 2001. (Yoshizaki et al., 2001)

In this paper, inner structures of a polar low, which

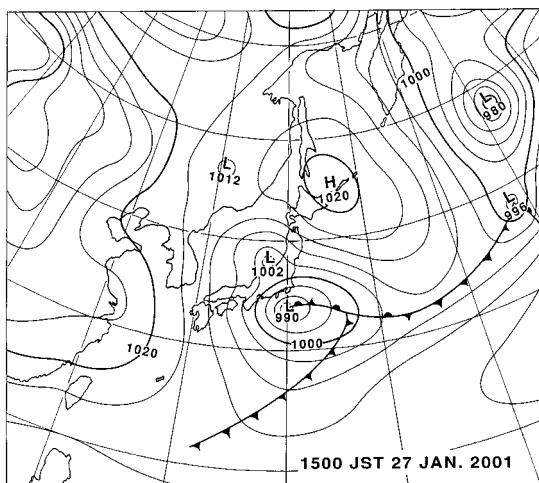


Fig. 1 Surface weather map at 15 JST on 27 Jan. 2001.

\*Corresponding author's address : Masataka Murakami, Meteorological Research Institute, Tsukuba, Ibaraki 305-0052, Japan; E-Mail: [mamuraka@mri-jma.go.jp](mailto:mamuraka@mri-jma.go.jp)

appeared over the Japan Sea on 27 Jan., are documented mainly on the basis of in-situ measurements, cloud radar observations and dropsonde sounding from an instrumented aircraft (Gulfstream-II).

## 2. OBSERVATION FACILITIES

In the 2001 field campaign "WMO-01", we flew an instrumented aircraft (Gulfstream-II). The instrumented aircraft provided us with data of microphysical, thermodynamic and kinetic structures in and around snow cloud systems. It also provided us with the w-band radar data (reflectivity and Doppler velocity) and GPS dropsonde data. Another aircraft (Citation-V) provided us with GPS dropsonde data around snow cloud systems observed by G-II. Ground-based observations deployed for this campaign included 4 portable X-band Doppler radars, two wind profilers and three additional aerological stations. Three observation ships of JMA also carried out upper-air soundings every three or six hours for

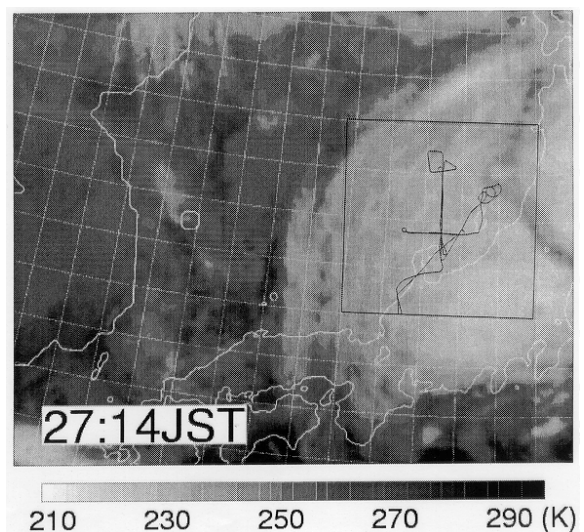


Fig. 2 GMS-5 IR image at 14JST on 27 Jan. 2001 and flight track of G-II.

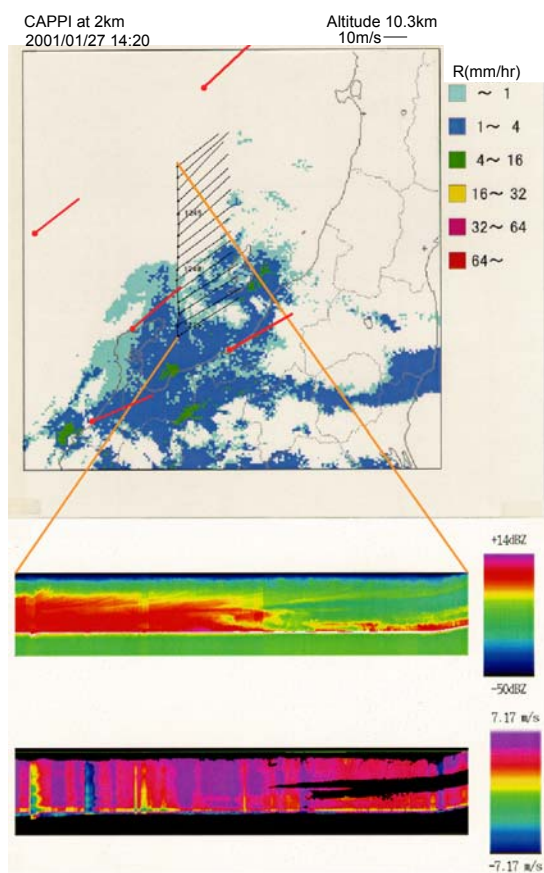


Fig. 3 G-II flight track of north bound leg at 10.3 km, 1-min averaged wind barbs, CAPPI of JMA's C-band radar composite at 2 km level at 1240 (upper panel) and vertical cross-section of reflectivity and Doppler velocity measured with the w-band cloud radar (middle and lower panel). No correction for attenuation by hydrometeors is applied.

this campaign.

### 3. SYNOPTIC AND MESOSCALE FEATURES

The polar low formed between Noto Peninsula and Sado Island over the Japan Sea when a synoptic-scale low passed by along the Pacific coast of the Japan Islands during the daytime on Jan. 27. Then the polar low moved slowly northeastward and reached to the north of Sado Island by 2100 JST (Fig. 1).

The timing of the polar low formation was correspondent to the superposition of a low pressure region at 700 hPa level, which was moving southeastward from central parts of the Japan Sea to the Pacific Ocean. The echo areas associated with the polar low showed circular/spiral-shaped pattern and

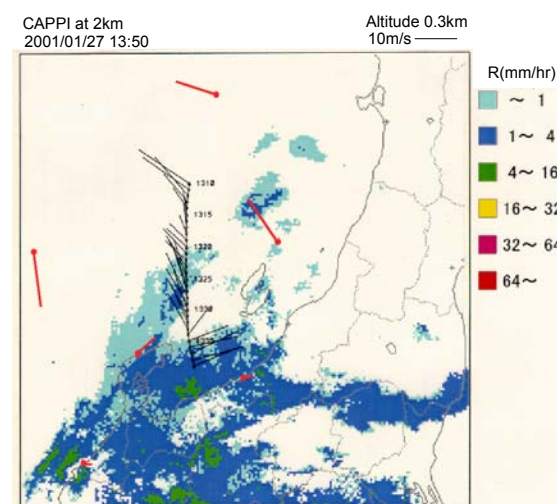
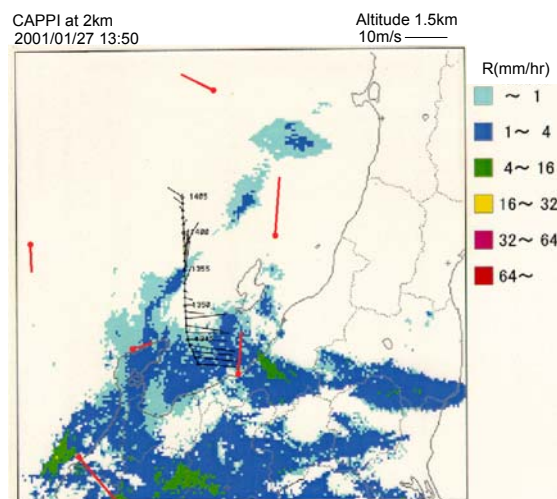
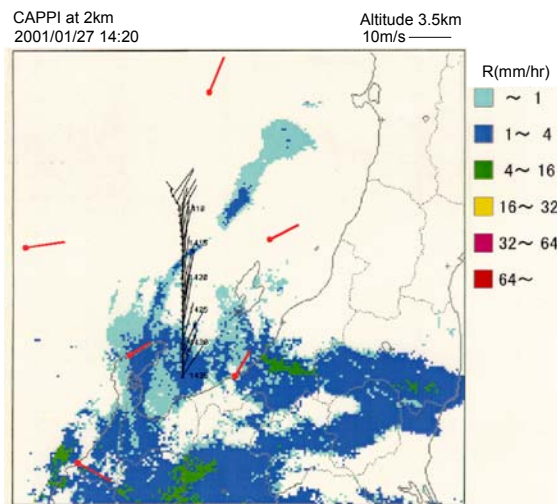


Fig. 4 G-II flight track, 1-min averaged wind barbs observed by aircraft, wind barbs at 0.3, 1.5 and 3.5km observed with rawinsondes and dropsondes, superposed with CAPPI at 2km level at times closest to each flight leg.

were quasi-stationary during the aircraft observation period (from 1230 to 1600 JST), although they were weak in intensity.

#### 4. OBSERVATIONAL RESULTS

We flew the instrumented aircraft on four legs at different heights (10.3, 3.6, 1.5 and 0.3 km) along the longitude line of 137.5E, and two legs at different heights (10.2 and 1.5 km) along the latitude line of 37.7N. In-situ observations of kinetic, thermodynamic and microphysical structures in/around the cloud system were made as well as measurements of reflectivity and Doppler velocity with the w-band cloud radar and soundings with GPS dropsonde.

Upper-level clouds associated with the synoptic-scale low extended widely over the observation area and the polar low was not identified in the satellite images during the aircraft observation period (Fig. 2).

At 10.3 km level, horizontal winds were rather uniform and southwesterly with a speed of  $\sim 30 \text{ ms}^{-1}$ . Cloud radar indicated that upper-level stratiform clouds associated with the synoptic-scale low existed between 4~9 km and lower-level clouds associated with the polar low were seen beneath the upper-level

clouds and their tops reached the heights of 3~4 km.

As seen from Fig. 4, horizontal winds showed remarkable spatial change below 1.5 km level. Especially at 0.3 km, the easterly winds with a speed greater than  $10 \text{ ms}^{-1}$  were on the northern side and westerly winds on the southern side. Such a cyclonic wind pattern was not found at 3.5 km level.

The warm core was found in the central/southern parts (DISTANCE= -30~-100km) of the polar low. Temperature contrast was most prominent at 1.5 km level and equivalent potential temperature was higher by 2~3 degrees than its surroundings at this level (Fig. 5).

Figure 6 shows that on the average, weak updraft ( $10\sim 30 \text{ cms}^{-1}$ ) existed in the central/southern parts (DISTANCE=0~80 km) of the polar low below 1.5 km level although actual vertical wind field mingles updraft and downdraft in horizontal scales of  $10\sim 20 \text{ km}$ .

Pressure dip of 1~2 hPa was found in the central/southern parts of the polar low at 0.3 km level on the basis of difference between pressure heights and GPS heights.

Figure 7 shows horizontal distribution of equivalent potential temperature and horizontal wind at 1.5 km level, which is derived from the interpolation of observed data. As parts of the circulation associated with the synoptic-scale low, airmass with high  $\theta_e$

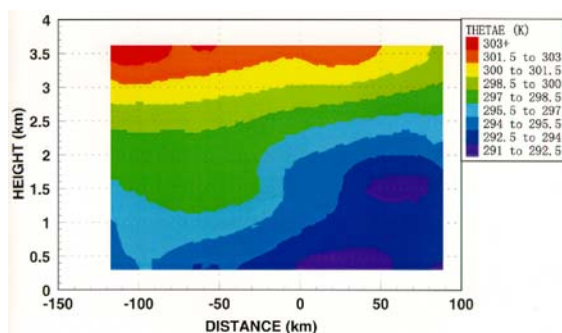


Fig. 5 Vertical cross section of equivalent potential temperature along the longitude line of 137.5E. Distance increases with moving northward.

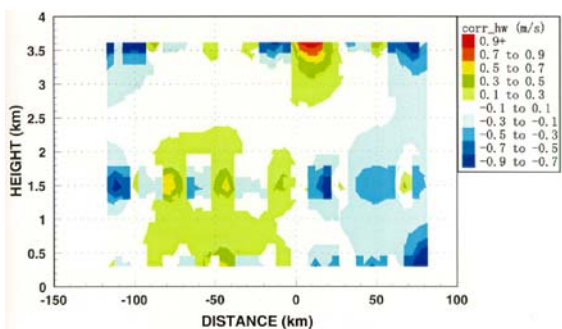


Fig. 6 Vertical cross section of vertical velocity along the longitude line of 137.5E.

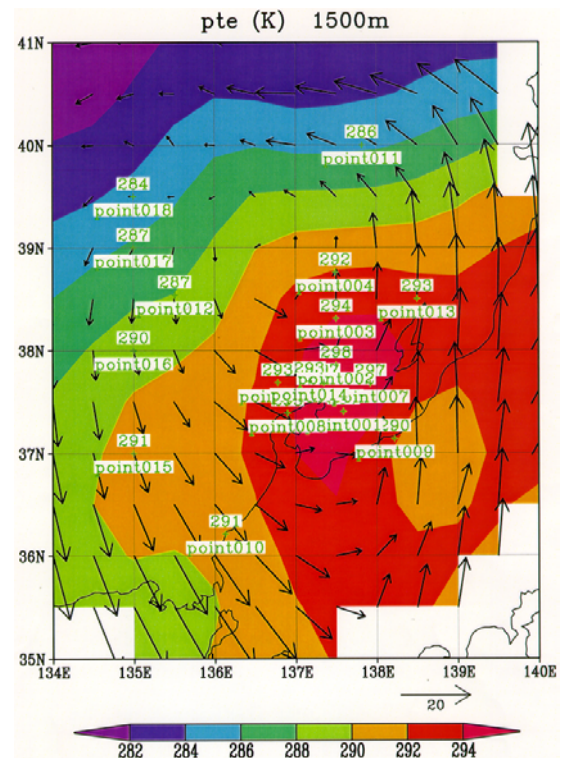


Fig. 7 Horizontal distribution of equivalent potential temperature and horizontal winds at 1.5 km level.

entered the domain through southeast boundaries and went out from the domain through southwest boundaries. Figure 7 suggested that parts of the circulation associated with the synoptic-scale low formed a secondary cyclonic circulation and the warm core existed around the center of the secondary circulation.

Higher concentrations of ice crystals and snow particles measured with 2D-C probe were found on the both side of the weak updraft region, where horizontal gradient of  $\theta_e$  was large (Fig. 8). Cloud droplet regions with low water contents ( $0.1 \sim 0.2 \text{ gm}^{-3}$  at most) were almost collocated with the snow particle regions with higher concentrations (Fig. 9).

Excess vapor produced by the polar low's circulation was consumed by the depositional growth of ice crystals seeded from the upper cloud deck associated with the synoptic-scale low. Therefore cloud droplet regions were confined to below 1.5 km level except for the northern part (DISTANCE =  $60 \sim 80 \text{ km}$ ) where concentrations of ice and snow particles were very low.

## 5. SUMMARY

The organized cloud system associated with the polar low, which formed between Noto Peninsula and Sado Island over the Japan Sea, on 27 January 2001, were investigated mainly with an instrumented aircraft (Gulfstream- II).

Mesoscale structures of the polar low, which is derived on a basis of in-site measurement, cloud radar observation and dropsonde sounding from G-II as well as ground-based radar observations, rawinsonde sounding from additional aerological stations and observation ships and Citation-V's dropsonde sounding, are shown in Fig 10.

The cloud system had the horizontal scale of  $100 \sim 200 \text{ km}$  and vertical scale of  $3 \sim 4 \text{ km}$ . Characteristic wind fields were detected below the height of 1.5 km. Remarkable cyclonic wind patterns were found at the lowest level (0.3 km). The warm core was most remarkable at 850 hPa level and  $\theta_e$  in the warm core was higher by  $2 \sim 3$  degrees than its surroundings. Neither the cyclonic circulation nor the warm core were found at 700 hPa level.

Most of excess vapor produced by the polar low circulation was consumed through the deposition of ice crystals seeded from upper clouds associated with the synoptic-scale low passed by along the Pacific coast of the Japan Islands. As a result, cloud droplet regions were spatially and temporally limited and their water contents were  $0.1 \sim 0.2 \text{ gm}^{-3}$  at most. The

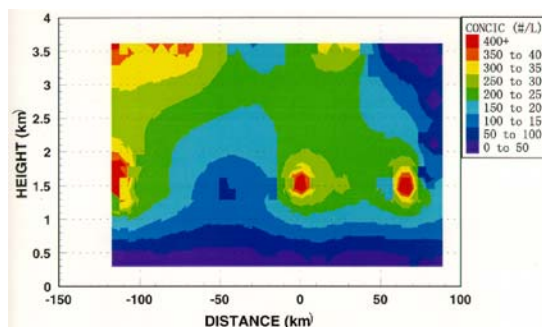


Fig. 8 Vertical cross section of snow particle concentrations measured with 2D-C probe along the longitude line of 137.5E.

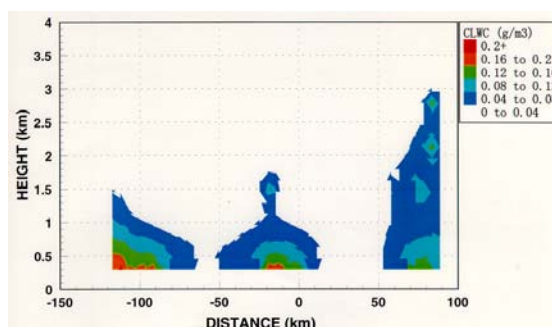


Fig. 9 Vertical cross section of cloud water contents along the longitude line of 137.5E.

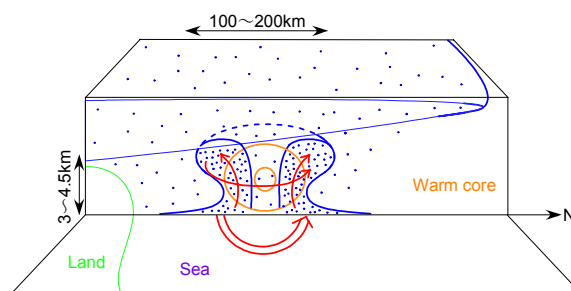


Fig. 10 Schematic of mesoscale structures of a polar low observed on 27 Jan. 2001.

primary growth mechanism of precipitation particles was the depositional growth of ice and snow particles and accretional growth of snow particles was the secondary mechanism in this cloud system.

## 6. REFERENCES

- Yoshizaki, M., T. Kato, H. Eito, M. Murakami, S. Hayashi and WMO-01 group, 2001: A report on a field experiment " winter MCSs (mesoscale convective systems) observations over the Japan Sea in January 2001(WMO-01). Preprint of International Conference on Mesoscale Meteorology and Typhoon in East Asia, 370-373.